J|A|C|S

A R T I C L E S

The Role of Outer-Sphere Surface Acidity in Alkene Epoxidation Catalyzed by Calixarene−Ti(IV) Complexes

Justin M. Notestein,[†,§] Andrew Solovyov,[†] Leandro R. Andrini,[‡] Felix G. Requejo,[‡] Alexander Katz,*,[†] and Enrique Iglesia*,[†]

Contribution from the Department of Chemical Engineering, University of California at Berkeley, Berkeley, California 94720, and INIFTA e IFLP (CONICET), Facultad de Ciencias Exactas, Universidad Nacional de La Plata, 1900 La Plata, Argentina

Received June 23, 2007; E-mail: askatz@berkeley.edu; iglesia@berkeley.edu

Abstract: Cooperativity between Brønsted acidic defect sites on oxide surfaces and Lewis acid catalyst sites consisting of grafted calixarene−Ti(IV) complexes is investigated for controlling epoxidation catalysis. Materials are synthesized that, regardless of the surface or calixarene substituent, demonstrate nearly identical UV−visible ligand-to-metal charge-transfer bands and Ti K-edge X-ray absorption near edge spectral features consistent with site-isolated, coordinatively unsaturated Ti(IV) atoms. Despite similar Ti frontier orbital energies demonstrated by these spectra, replacing a homogeneous triphenylsilanol ligand with a silanol on a SiO_2 surface increases cyclohexene epoxidation rates with *tert*-butyl hydroperoxide 20-fold per Ti site. Supporting calixarene−Ti active sites on fully hydroxylated Al_2O_3 or TiO_2, which possess lower average surface hydroxyl pK_a than that of SiO_2, reduces catalytic rates 50-fold relative to SiO_2. These effects are consistent with SiO_2 surfaces balancing two competing factors that control epoxidation rates— equilibrated hydroperoxide binding at Ti, disfavored by stronger surface Brønsted acidity, and rate-limiting oxygen transfer from this intermediate to alkenes, favored by strongly H-bonding intermediates. These observations also imply that Ti−OSi rather than Ti-OCalix bonds are broken upon hydroperoxide binding to Ti in kinetically relevant steps, which is verified by the lack of a calixarene upper-rim substituent effect on epoxidation rate. The pronounced sensitivity of observed epoxidation rates to the support oxide, in the absence of changes to the Ti coordination environment, provides experimental evidence for the importance of outer-sphere H-bonding interactions for the exceptional epoxidation reactivity of titanium silicalite and related catalysts.

Introduction

The design and characterization of solid catalysts at the atomic level is challenging, at least in part because of the difficulty in deconvoluting inner- and outer-sphere effects on their catalytic function.[1,2] Inner-sphere effects arise from ligands coordinated directly to active atoms and consequent changes to the ground-state electronic structure of these atoms. The outer-sphere is less well-defined for inorganic solid catalysts and consists of noncoordinated moieties, such as vicinal Brønsted acid sites, coadsorbed species, and the fluid phase.

Titanosilicates, such as TS-1, represent a class of materials for which atomic-level details are only gradually emerging, despite their broad application as epoxidation catalysts.[3] The accepted mechanism for epoxidation of unfunctionalized alkenes on all Ti−SiO_2 materials involves concerted oxygen transfer from an electrophilic oxygen on Ti-bound hydroperoxides to the alkene substrate.[4−7] In other epoxidation systems, reaction rates have been shown to increase with increasing electrophilicity of stoichiometric oxidants[8] and homogeneous catalysts.[9] Therefore, the superior alkene epoxidation properties of Ti−SiO_2 relative to other molecular and supported metal oxides,[10] have been primarily attributed to an inner-sphere effect of coordinatively unsaturated tetrahedral Ti atoms stabilized within an electronegative SiO_2 framework. This assignment of the active structure is consistent with theoretical calculations,[11−17]

† University of California.

‡ Universidad Nacional de La Plata.

§ Current address: Department of Chemical and Biological Engineering, Northwestern University, Evanston IL 60208.

(1) Corma, A. *Catal. Rev. Sci. Eng.* **2004**, *46*, 369−417.

(2) Notestein, J. M.; Katz, A. *Chem. Eur. J.* **2006**, *12*, 3954−3965.

(3) Clerici, M. G.; Bellussi, G.; Romano, U. *J. Catal.* **1991**, *129*, 159−167. Notari, B. *Adv. Catal.* **1996**, *41*, 253−334. Sheldon, R. A.; Wallau, M.; Arends, I. W. C. E.; Schuchardt, U. *Acc. Chem. Res.* **1998**, *31*, 485−493. Saxton, R. J. *Top. Catal.* **1999**, *9*, 43−57. Corma, A. *J. Catal.* **2003**, *216*, 298−312.

(4) Sheldon, R. A.; van Doorn, J. A. *J. Catal.* **1973**, *31*, 427−437.

(5) Sheldon, R. A.; van Doorn, J. A.; Schram, C. W. A.; De Jong, A. J. *J. Catal.* **1973**, *31*, 438−443. Khouw, C. B.; Dartt, C. B.; Labinger, J. A.; Davis, M. E. *J. Catal.* **1994**, *149*, 195−205; Corma, A.; Garcia, H. *Chem. Rev.* **2002**, *102*, 3837−3892.

(6) Sheldon, R. A. *J. Mol. Catal.* **1980**, *7*, 107−126.

(7) Oldroyd, R. D.; Thomas, J. M.; Maschmeyer, T.; MacFaul, P. A.; Snelgrove, D. W.; Ingold, K. U.; Wayner, D. D. M. *Angew. Chem., Int. Ed. Engl.* **1996**, *35*, 2787−2790.

(8) Lynch, B. M.; Pausacker, K. H. *J. Chem. Soc.* **1955**, 1525−1531. Medvedev, S.; Blokh, O. *J. Phys. Chem. USSR* **1933**, *4*, 721−730.

(9) Palucki, M.; Finney, N. S.; Pospisil, P. J.; Güler, M. L.; Ishida, T.; Jacobsen, E. N. *J. Am. Chem. Soc.* **1998**, *120*, 948−954. Cavallo, L.; Jacobsen, H. *J. Org. Chem.* **2003**, *68*, 6202−6207.

(10) Wulff, H. P.; Wattimena, F. (Shell Oil Company) 1978. Nemeth, L. T.; Malloy, T. P.; Jones, R. R. (UOP) 1995.
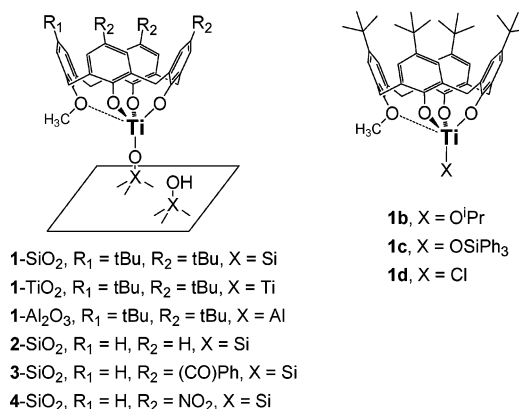
(11) Neurock, M.; Manzer, L. E. *Chem. Commun.* **1996**, 1133−1134.

(12) Sinclair, P. E.; Catlow, C. R. A. *J. Phys. Chem. B* **1999**, *103*, 1084−1095.

UV−visible spectroscopy studies,[18,19] and X-ray absorption spectroscopy studies.[20,21] The basis for the marked differences in epoxidation rates, optimal conditions, and preferred oxidants between TS-1 and other titanosilicates,[22] Ti−SiO$_2$ materials,[23] and homogeneous complexes,[24] however, remains controversial,[25,26] particularly because all effective catalysts show similar Ti inner-sphere environments by the aforementioned electronic spectroscopies.

H-bonding assemblies of outer-sphere Brønsted acids have been proposed as intermediates in epoxidation catalysis on TS-1 to explain the strong effects of protic solvents on rates.[27] These rate increases could not be explained solely on the basis of adsorption and partitioning.[26,28] The presence of Brønsted acidic silanol nests[15] or silanols generated by hydroperoxide binding,[11] alone or in combination with protic solvents, has been suggested to explain differences between the reactivity of TS-1 and other Ti catalysts. However, experimental proof of an outer-sphere effect in TS-1 catalysis has remained elusive, at least in part, because of the difficulty in identifying which bond-breaking processes form Brønsted acids in the kinetically relevant steps,[29,30] and because systematic and proven variations of the inner- and outer-spheres are difficult to achieve in heterogeneous

Scheme 1. Overview of Surface-Grafted and Homogeneous Calixarene−Ti Complexes

1-SiO$_2$, R$_1$ = tBu, R$_2$ = tBu, X = Si
1-TiO$_2$, R$_1$ = tBu, R$_2$ = tBu, X = Ti
1-Al$_2$O$_3$, R$_1$ = tBu, R$_2$ = tBu, X = Al
2-SiO$_2$, R$_1$ = H, R$_2$ = H, X = Si
3-SiO$_2$, R$_1$ = H, R$_2$ = (CO)Ph, X = Si
4-SiO$_2$, R$_1$ = H, R$_2$ = NO$_2$, X = Si

1b, X = O^{i}Pr
1c, X = OSiPh$_3$
1d, X = Cl

catalysts without unintended changes in structural features of uncertain importance to catalytic function.[31]

Here, electron-donating and electron-withdrawing calixarenes (macrocyclic phenols **1a**−**4a**) are synthesized and molecular calixarene−Ti complexes are grafted covalently to oxide surfaces (Scheme 1: SiO$_2$, TiO$_2$, Al$_2$O$_3$, and triphenylsilanol as a model) to address the kinetic relevance of outer-sphere Brønsted acidity on Ti-catalyzed cyclohexene epoxidation with *tert*-butylhydroperoxide. The Ti inner-sphere environment remains constant, as probed by ligand-to-metal charge transitions (LMCT) in the UV−visible spectrum and by Ti 1s−3d electronic transitions that give rise to near-edge features in the Ti K-edge absorption spectrum. In contrast, calixarene phenols and oxide support OH defects are chosen to span a broad pK_a range. Therefore, the sensitivity of the observed epoxidation rate to ligand or support variations probes the kinetic relevance of Brønsted acids formed from Ti−O-support or Ti−O-calixarene bond cleavage.

We have previously demonstrated that calixarene−Ti complexes grafted covalently on SiO$_2$ are single-site heterogeneous catalysts for epoxidation of alkenes with organic hydroperoxides.[32] The single-site nature of these catalysts eliminates the confounding effects of ensemble-averaging in structural and functional characterization, in contrast with the nonuniform active sites that can arise from post-synthesis modifications of Ti centers[33] or doping of support oxides.[34] Grafted calixarene−Ti catalysts are also more active than samples prepared by removing their organic ligands by thermal treatment in air (material **1**-SiO$_2$-**c**) or Ti−SiO$_2$ samples prepared by alkoxide grafting at similar Ti surface densities.[35] The multidentate and bulky calixarene−Ti precursors enforce site isolation during synthesis and during reaction and organize phenolate ligands to create Ti Lewis centers stronger than those formed

(13) Yudanov, I. V.; Gisdakis, P.; Di, Valentin, C.; Rosch, N. *Eur. J. Inorg. Chem.* **1999**, *12*, 2135−2145.
(14) Sever, R. R.; Root, T. W. *J. Phys. Chem. B* **2003**, *107*, 4090−4099.
(15) Wells, D. H.; Delgass, W. N.; Thomson, K. T. *J. Am. Chem. Soc.* **2004**, *126*, 2956−2962. Wells, D. H.; Joshi, A. M.; Delgass, W. N.; Thomson, K. T. *J. Phys. Chem. B* **2006**, *110*, 14627−14639.
(16) Vayssilov, G. N.; van Santen, R. A. *J. Catal.* **1998**, *175*, 170−174.
(17) Urakawa, A.; Burgi, T.; Skrabal, P.; Bangerter, F.; Baiker, A. *J. Phys. Chem. B* **2005**, *109*, 2212−2221.
(18) Geobaldo, F.; Bordiga, S.; Zecchina, A.; Giamello, E.; Leofanti, G.; Petrini, G. *Catal. Lett.* **1992**, *16*, 109−115. Bellussi, G.; Rigutto, M. S. *Stud. Surf. Sci. Catal.* **1994**, *85*, 177−213. Klein, S.; Thorimbert, S.; Maier, W. F. *J. Catal.* **1996**, *163*, 476−488. Marchese, L.; Maschmeyer, T.; Gianotti, E.; Coluccia, S.; Thomas, J. M. *J. Phys. Chem. B* **1997**, *101*, 8836−8838. Soult, A. S.; Poorè, D. D.; Mayo, E. I.; Stiegman, A. E. *J. Phys. Chem. B* **2001**, *105*, 2687−2693. Bonino, F.; Damin, A.; Ricchiardi, G.; Ricci, M.; Spanò, G.; D'Aloisio, R.; Zecchina, A.; Lamberti, C.; Prestipino, C.; Bordiga, S. *J. Phys. Chem. B* **2004**, *108*, 3573−3583. Fraile, J. M.; Garcia, J. I.; Mayoral, J. A.; Vispe, E. *J. Catal.* **2005**, *233*, 90−99.
(19) Gao, X.; Bare, S. R.; Fierro, J. L. G.; Banares, M. A.; Wachs, I. E. *J. Phys. Chem. B* **1998**, *102*, 5653−5666.
(20) Blanco-Brieva, G.; Capel-Sanchez, M. C.; Campos-Martin, J. M.; Fierro, J. L. G.; Lede, E. J.; Adrini, L.; Requejo, F. G. *Adv. Synth. Catal.* **2003**, *345*, 1314−1320. Bordiga, S.; Coluccia, S.; Lamberti, C.; Marchese, L.; Zecchina, A.; Boscherini, F.; Buffa, F.; Genoni, F.; Leofanti, G.; Petrini, G.; Vlaic, G. *J. Phys. Chem.* **1994**, *98*, 4125−4132. Davis, R. J.; Liu, Z.; Tabora, J. E.; Wieland, W. S. *Catal. Lett.* **1995**, *34*, 101. Fraile, J. M.; García, J. I.; Mayoral, J. A.; Proietti, M. G.; Sánchez, M. C. *J. Phys. Chem.* **1996**, *100*, 19484−19488. Imamura, S.; Nakai, T.; Kanai, H.; Shiono, T.; Utano, K. *Catal. Lett.* **1996**, *39*, 79−82.
(21) Thomas, J. M.; Sankar, G. *Acc. Chem. Res.* **2001**, *34*, 571−581.
(22) Blasco, T.; Camblor, M. A.; Corma, A.; Pariente, J. P. *J. Am. Chem. Soc.* **1993**, *115*, 11806−11813; Reddy, J. S.; Kumar, R.; Ratnasamy, P. *Appl. Catal.* **1990**, *58*, L1−L4.
(23) Maschmeyer, T.; Rey, F.; Sankar, G.; Thomas, J. M. *Nature* **1995**, *378*, 159−162. Blasco, T.; Corma, A.; Navarro, M. T.; Pariente, J. P. *J. Catal.* **1995**, *156*, 65−74. Cativiela, C.; Fraile, J. M.; García, J. I.; Mayoral, J. A. *J. Mol. Catal.* **1996**, *112*, 259−267. Corma, A.; Díaz, U.; Fornés, V.; Jordá, J. L.; Domine, M.; Rey, F. *Chem. Commun.* **1999**, 779−780. Deng, Y.; Maier, W. F. *J. Catal.* **2001**, *199*, 115−122.
(24) Johnson, B. F. G.; Klunduk, M. C.; Martin, C. M.; Sankar, G.; Teate, S. J.; Thomas, J. M. *J. Organomet. Chem.* **2000**, *596*, 221−225. Beck, C.; Mallat, T.; Baiker, A. *New J. Chem.* **2003**, *27*, 1284−1289.
(25) Sastre, G.; Corma, A. *Chem. Phys. Lett.* **1999**, *302*, 447−453. Adam, W.; Corma, A.; García, H.; Weichold, O. *J. Catal.* **2000**, *196*, 339−344.
(26) Clerici, M. G. *Top. Catal.* **2001**, *15*, 257−263. Clerici, M. G. *Oil Gas* **2006**, *32*, 77−82.
(27) Bellussi, G.; Carati, A.; Clerici, M. G.; Maddinelli, G.; Millini, R. *J. Catal.* **1992**, *133*, 220−230. Clerici, M. G.; Ingallina, P. *J. Catal.* **1993**, *140*, 71−83. Corma, A.; Esteve, P.; Martínez, A. *J. Catal.* **1996**, *161*, 11−19.
(28) Langhendries, G.; De Vos, D. E.; Baron, G. V.; Jacobs, P. A. *J. Catal.* **1999**, *187*, 453−463.
(29) Crocker, M.; Herold, R. H. M.; Orpen, A. G.; Overgaag, M. T. A. *J. Chem. Soc., Dalton Trans.* **1999**, 3791−3804.
(30) Ikeue, K.; Ikeda, S.; Watanabe, A.; Ohtani, B. *Phys. Chem. Chem. Phys.* **2004**, *6*, 2523−2528. Lin, W. Y.; Frei, H. *J. Am. Chem. Soc.* **2002**, *124*, 9292−9298.

(31) We do not discuss here the role of surface Brønsted acidity in leading to undesired epoxide ring opening in the presence of water or other primary alcohols. This side reaction is eliminated here by strictly anhydrous process conditions and does not arise from cooperative interactions between the Ti active site and surface OH defects.
(32) Notestein, J. M.; Iglesia, E.; Katz, A. *J. Am. Chem. Soc.* **2004**, *126*, 16478−16486.
(33) Fraile, J. M.; García, J. I.; Mayoral, J. A.; Vispe, E. *J. Catal.* **2000**, *189*, 40−51. Fraile, J. M.; García, J. I.; Mayoral, J. A.; Salvatella, L.; Vispe, E.; Brown, D. R.; Fuller, G. *J. Phys. Chem. B* **2003**, *107*, 519−526. Brutchey, R. L.; Ruddy, D. A.; Anderson, L. K.; Tilley, T. D. *Langmuir* **2005**, *21*, 9576−9583.
(34) Oldroyd, R. D.; Sankar, G.; Thomas, J. M.; Özkaya, D. *J. Phys. Chem. B* **1998**, *102*, 1849−1855. Thomas, J. M.; Sankar, G.; Klunduk, M. C.; Attfield, M. P.; Maschmeyer, T.; Johnson, B. F. G.; Bell, R. G. *J. Phys. Chem. B* **1999**, *103*, 8809−8813.
(35) See Supporting Information for further discussion.

from alkoxy precursors.[36,37] We have recently shown that the calixarene macrocycle controls the oxygen coordination at the grafted Ti atom without perturbing the isolated nature of active Ti atoms.[38]

Experimental Methods

General Analytical. The mass loss of all grafted calixarene materials was determined by thermogravimetry (TGA; TA Instruments 2950) in a flow of dry synthetic air (2.0 cm^3 s^{-1} 3:1 N$_2$:O$_2$ from vaporized liquid O$_2$ and N$_2$ at a heating rate of 0.083 K s^{-1}) after correction for hydroxyl condensation losses (determined from mass losses in unmodified supports). Calixarene contents were estimated by assuming that mass losses reflect combustion of a molecular weight of 612 g/mol site (C$_{45}$H$_{55}$O) in material **1** and were adjusted accordingly for other upper-rim substituted grafted calixarenes. Ti inductively coupled plasma emission mass spectrometry (ICP/MS) was performed by Quantitative Technologies, Inc.

UV−visible spectra were measured at ambient conditions using a Cary 400 Bio UV−visible spectrophotometer (Varian) equipped with a Harrick Praying Mantis diffuse reflectance accessory. Pressed poly-(tetrafluoroethylene) powders were used as perfect reflector standard in calculating Kubelka−Munk pseudoabsorbances. The edge energies were calculated by assuming that the lowest energy transitions (calixarene−Ti LMCT) were indirect.[39] Tangent lines as shown in Figure 2 were calculated from the first derivatives of the transformed sample spectra. Solid-state ^{1}H magic angle spinning (MAS) and ^{13}C cross-polarized magic angle spinning (CP/MAS) NMR spectra were collected using a Bruker DSX500 spectrometer operating at 500 MHz at the Caltech Solid-State NMR facility. Solution NMR spectra were measured using a Bruker AMX400 spectrometer operating at 400 MHz at the UC-Berkeley NMR facility.

Ti K-Edge X-ray Absorption Near Edge Spectroscopy (XANES). Ti K-edge XANES were measured using a Si(111) single-crystal monochromator and a multielement fluorescence detector held within a sample holder with pressure and temperature control (incident beam energy of 1.37 MeV, < 1% harmonics; 0.8 eV resolution; Laboratorio Nacional de Luz Sincrotrón; D04B-XAS beamline; LNLS, Campinas, Brazil). Photon energies were calibrated in transmission mode using a Ti foil by setting the first inflection point in its spectrum at its known absorption edge (4966 eV).[40] Background contributions were removed by fitting the region below 4960 eV to a fourth-order polynomial (Victoreen). Pre-edge features with maxima at 4968−4970 eV were fitted using four Gaussian peaks (A1, A2, A3, and B in order of increasing energy).

The four pre-peaks, assigned as A1, A2, A3, and B, correspond to transitions from the 1s core electron to Ti 3d-4p-4s hybridized states. The A1 pre-peak arises from a t$_{2g}$ bandlike state, whereas A2 and A3 features reflect e$_g$ bandlike states. The t$_{2g}$ and e$_g$ states represent the components of the crystal-field split Ti-3d atomic orbitals, which are shifted in energy relative to each other as a result of the oxygen environment surrounding the Ti center.[41] In the particular case of anatase TiO$_2$, the A1 feature mainly arises from perturbations by the first shell

of four Ti neighbors at 3.04 Å, while the intensity of A2 and A3 peaks is assigned to the transitions due to perturbation by the second set of Ti neighbors at 3.78 Å.[42] The Ti-3d atomic orbitals influence each other via hybridization with oxygen orbitals located between them. Transition B has a predominantly Ti-4p character, but is hybridized with the Ti-4s and/or O-2p orbitals.[43]

The relative area of the combined A2 and A3 features is reported here as a measure of the availability of unoccupied electronic states at the Ti 3d level, which decreases with the Ti average coordination number. In particular, it is greatest for isolated tetrahedral Ti centers. This area has been shown to be a useful descriptor of epoxidation turnover rates for a wide range of electronic environments in Ti−SiO$_2$ materials.[38] Spectra were normalized by the average X-ray absorption intensity of the sample between 5050 and 5200 eV. Detailed procedures and analyses have been reported elsewhere.[38] All samples were treated in situ at 383 K in a vacuum of ∼10^{-6} Torr during X-ray absorption experiments.

Calixarene Synthesis Protocols. The syntheses of calixarene ligands and calixarene−Ti complexes (Scheme 2) were conducted using standard Schlenk-line conditions. The solvents and reagents used were the highest available purity (Aldrich); they were dried and distilled using standard methods before use.[44] **1a** and **2a** were synthesized from iodomethane and *tert*-butylcalix[4]arene **1** and calix[4]arene **2**, respectively.[45] Calix[4]arene **2** was synthesized from **1** via reaction with phenol in the presence of AlCl$_3$ in toluene.[46] New compounds **3a** and **4a** were synthesized from **2a** via modified Friedel−Crafts procedures described in the Supporting Information. These procedures led to selective substitution at the para position of free phenols and isolation of the desired "cone" conformation shown in Scheme 2. This "cone" conformation was confirmed from its methylene ^{13}C NMR resonances at ∼31.5 ppm.[47]

Ti Complex and Grafted Materials Synthesis. Complex **1d** (Scheme 1) was synthesized from calixarene **1a** and bis(tetrahydrofuran)-TiCl$_4$, as reported previously.[48] Complexes **1b**,[49] **2b**, **3b**, and **4b** (Scheme 2) were synthesized by adding 1 equiv Ti(O^{i}Pr)$_4$ (Aldrich 99.999%) to a 0.1 M solution of **1a**−**4a** in toluene and then stirring under a N$_2$ atmosphere for 48 h at ambient temperature. Complexes **1b** and **2b** were isolated by evaporating solvents to form red glassy and dull orange solids, respectively. Complexes **3b** and **4b** could not be isolated successfully as analytically pure species because of their low solubility. Complexes **1c** and **2c** were prepared by adding 0.1 M solutions of **1b** or **2b** in toluene to 1 equiv triphenylsilanol and refluxing 24 h in N$_2$ flow. The evaporation of volatile species at ambient temperature produced analytically pure **1c** as an orange solid. Analytically pure yellow powders of **2c** were obtained after evaporation of the synthesis solution and washing with anhydrous hexane. Detailed characterization data for these complexes are provided in the Supporting Information.

Mesoporous SiO$_2$ (Selecto Scientific) consists of 250−500 μm diameter aggregates with ∼6.0 nm average diameter pores, possesses a N$_2$ BET surface area of 498 m^2/g^{-1}, and produces pH ∼7 as a 5% suspension in H$_2$O. Hombikat UV100 TiO$_2$ (Sachtleben) consists of 12 nm anatase crystallites embedded within 50 nm primary particles, which further form ∼15 μm agglomerates possessing only macropores and a N$_2$ BET surface area of 343 m^2 g^{-1}. Al$_2$O$_3$ (Brockman I; CAMAG

(36) Nielson, A. J.; Schwerdtfeger, P.; Waters, J. M. *Dalton Trans.* **2000**, 529−537.
(37) Fantacci, S.; Sgamellotti, A.; Re, N.; Floriani, C. *Inorg. Chem.* **2001**, *40*, 1544−1549.
(38) Notestein, J. M.; Andrini, L. R.; Kalchenko, V. I.; Requejo, F. G.; Katz, A.; Iglesia, E. *J. Am. Chem. Soc.* **2007**, *129*, 1122−1131.
(39) Delgass, W. N.; Haller, G. L.; Kellerman, R.; Lunsford, J. H. *Spectroscopy in Heterogeneous Catalysis*; Academic Press: New York, 1979. Barton, D. G.; Shtein, M.; Wilson, R. D.; Soled, S. L.; Iglesia, E. *J. Phys. Chem. B* **1999**, *103*, 630−640. Argyle, M. D.; Chen, K. D.; Resini, C.; Krebs, C.; Bell, A. T.; Iglesia, E. *J. Phys. Chem. B* **2004**, *108*, 2345−2353.
(40) Waychunas, G. A. *Am. Miner.* **1987**, *72*, 89−101. Farges, F.; Brown, G. E.; Rehr, J. J. *Phys. Rev. B* **1997**, *56*, 1809−1819.
(41) Orgel, L. *An Introduction to Transition-Metal Chemistry. Ligand-field theory*; Methuen & Co. LTD.: London, 1964. Cotton, F. A. *Chemical Applications of Group Theory*; John Wiley and Sons, Inc.: New York, 1967.

(42) Wu, Z. Y.; Ouvrard, G.; Gressier, P.; Natoli, C. R. *Phys. Rev. B* **1997**, *55*, 10382−10391.
(43) Grunes, L. A. *Phys. Rev. B* **1983**, *27*, 2111−2131.
(44) Armarego, W. L. F.; Perrin, D. D. *Purification of Laboratory Chemicals*; 4th ed.; Butterworth-Heinemann: Boston, MA, 1996.
(45) Groenen, L. C.; Ruël, B. H. M.; Casnati, A.; Verboom, W.; Pochini, A.; Ungaro, R.; Reinhoudt, D. N. *Tetrahedron* **1991**, *47*, 8379−8384.
(46) Rathore, R.; Abdelwahed, S. H.; Guzei, I. A. *J. Am. Chem. Soc.* **2004**, *126*, 13582−13583.
(47) Jaime, C.; Demendoza, J.; Prados, P.; Nieto, P. M.; Sanchez, C. *J. Org. Chem.* **1991**, *56*, 3372−3376.
(48) Zanotti-Gerosa, A.; Solari, E.; Giannini, L.; Floriani, C.; Re, N.; Chiesi-Villa, A.; Rizzoli, C. *Inorg. Chim. Acta* **1998**, *270*, 298−311.
(49) Friedrich, A.; Radius, U. *Eur. J. Inorg. Chem.* **2004**, 4300−4316.

Scheme 2. Synthesis of Grafted Calixarene−Ti Materials
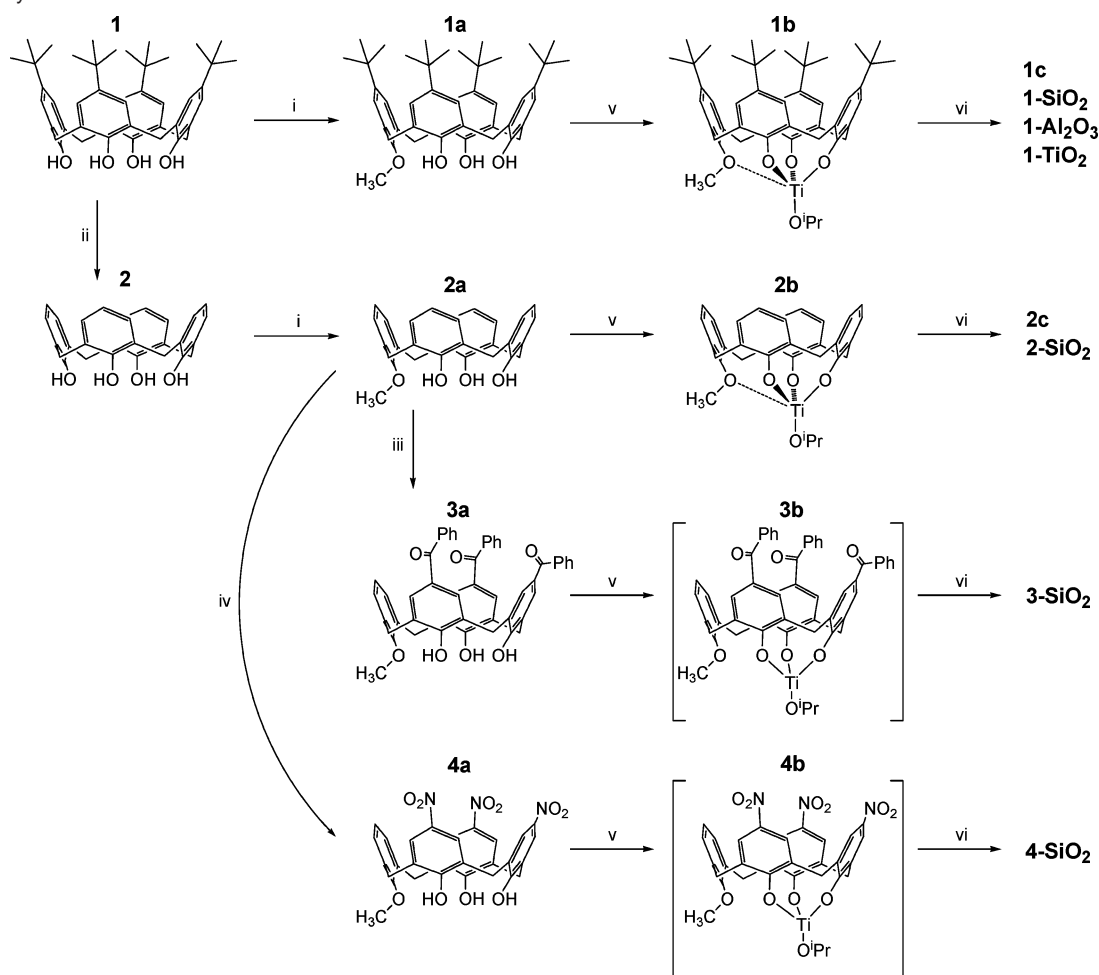
(i) 1.2 equiv CsF and 12 equiv iodomethane, anhydrous DMF, 333 K, 18 h; (ii) 4.8 equiv phenol and 5.3 equiv AlCl₃, toluene, 1 h room temp; (iii) 4.5 equiv AlCl₃ and 4 equiv benzyl chloride, toluene/nitrobenzene 10:1, 273 K, 0.75 h; (iv) 4.5 equiv KNO₃ and 6.8 equiv AlCl₃, acetonitrile, 273 K, 2 h; (v) 1 equiv TiOPr₄, toluene, 48 h room temp; (vi) 1 equiv Ph₃SiOH (**1c** or **2c**) or oxide surface, toluene, 24 h reflux. Compounds **3b** and **4b** were used directly in the synthesis of surface-grafted materials without intervening isolation.

Scientific) is a pseudo-boehmite phase material treated to 773 K during manufacture to remove 30% of its constitutional water resulting in a material with a N_2 BET surface area of 155 m² g⁻¹ and pH ~4.5 in a 5% suspension in H_2O. SiO_2 was treated in dynamic vacuum at 773 K for 24 h before grafting calixarene−Ti complexes. TiO_2 and Al_2O_3 were treated in dynamic vacuum at 393 K for 4 h before grafting calixarene−Ti species.

Surface-grafted complexes were synthesized by treating 0.1 M solutions or suspensions of **1b**−**4b** in toluene with the corresponding oxide support (0.25 mmol **1b**−**4b** per gram oxide) in sufficient additional toluene to fully suspend particles during magnetic stirring. Complexes **1b**−**4b** were used as synthesized without intervening purification steps. After adding **1b**−**4b**, suspensions were refluxed for 24 h, and the reactor was held at 388 K as N_2 was bubbled through the suspension until all volatiles were removed. The dry solids were washed with boiling toluene until calixarenes were no longer visible in the effluent and treated in dynamic vacuum for 4 h at ambient temperature. Material **1**-TiO_2 was protected from ambient light during synthesis and storage; all other materials were stored without specific precautions until use. Material **1**-SiO_2-**c** was prepared by treating **1**-SiO_2 at 823 K for 1 h in flowing N_2/O_2 (2.0 cm³ s⁻¹ 3:1 N_2:O_2) to remove all organic ligands by combustion. The UV−visible spectrum of catalyst **1**-SiO_2-**c** is similar to that of isolated Ti-oxo species on SiO_2 prepared by other means.[19]

Catalysis. Cyclohexene epoxidation rates and selectivities were measured by combining ~30 mg of catalyst and ~200 mg 4A molecular

sieves (previously dehydrated at 573 K under dynamic vacuum, 12 h) in a 25 mL sidearm flask and heating under dynamic vacuum for 1 h to the prescribed temperature indicated in the text (393−523 K). The flask was then backfilled with Ar and 20 mL of anhydrous *n*-octane (Aldrich, 99.8%, passed over SiO_2 and Al_2O_3 columns, freshly distilled off CaH_2) and 0.3 mL of cyclohexene (Aldrich, 99%, passed over Al_2O_3 column, freshly distilled off CaH_2) were added, and the reactor was sealed, magnetically stirred, and heated to 333 K. A solution of *tert*-butyl hydroperoxide (TBHP) in nonane (0.125 mL, 4.8 M solution in nonane with added 4A sieves, Aldrich) was added, and liquid aliquots were periodically removed and analyzed for reactants and products by gas chromatography (Agilent 6890, HP-1 methylsilicone capillary column) to measure catalytic reaction rates and selectivities. Solvents and reagents were kept rigorously dry to eliminate ring opening of epoxides catalyzed by Brønsted or Lewis acids. Neither diols nor other cyclohexene oxidation products were detected on SiO_2- and TiO_2-supported catalysts; less than one turnover to cyclohexane diol after 24 h was detected in reactions catalyzed by **1**-Al_2O_3. TBHP was used as the oxidant instead of the more reactive cumene hydroperoxide so as to minimize hydroperoxide decomposition (to acetone and phenol) in the presence of Brønsted acids.[50] Homogeneous catalysts were used at a concentration of ~0.2 mM, which led to the same total Ti atom

(50) Bewley, T.; Bowen, B. E. V.; Bramwyche, P. L.; Jackson, G. W. Hercules Powder Company: U.S.A., 1955. Wirth, M. M.; BP Chemicals Limited: U.S.A., 1979. Knifton, J. F.; Sanderson, J. R. *Appl. Catal. A* **1997**, *161*, 199−211.

Table 1. Physicochemical and Spectroscopic Data for Synthesized Materials and Complexes

material[a]			site density (nm^{-2})[b]		LMCT edge[c] (eV)	Ti K-edge XANES pre-edge[d]	
	R$_2$	X	Ti	calix		(eV)	($A_{A2} + A_{A3}$)/A_T
1b	^tBu	$^-O^iPr$	n/a	n/a	2.34[e]		
1c	^tBu	$^-OSiPh_3$	n/a	n/a	2.37[e]	4968.8	0.77
1-SiO$_2$	^tBu	SiO$_2$	0.24	0.24	2.21	4968.7	0.83
1-SiO$_2$-c		SiO$_2$	0.24		3.82[f]	4968.9	0.78
1-TiO$_2$	^tBu	TiO$_2$	n/a	0.19	2.18	n/a	n/a
1-Al$_2$O$_3$	^tBu	Al$_2$O$_3$	0.17	0.18[g]	2.18	4969.2	0.68
2-SiO$_2$	H	SiO$_2$	0.26	0.28	2.31		
3-SiO$_2$	(CO)Ph	SiO$_2$	0.19	0.17	2.26	4968.6	0.78
4-SiO$_2$	NO$_2$	SiO$_2$	0.18	0.22[g]	2.26	4968.9	0.75

[a] Labeled as per Scheme 1. [b] Determined by Ti ICP/MS or by TGA. [c] ± 0.02 eV. [d] Energy of pre-edge maximum ± 0.2 eV, component peak area ± 0.07. [e] Spectra acquired in chloroform solution. All materials spectra were collected in diffuse reflectance mode. [f] LMCT characteristic of Ti−O−Si. [g] Assumes additional combustion of four C$_3$H$_7$O surface groups per calixarene fragment; other materials assume additional combustion of 1 C$_3$H$_7$O surface group per calixarene fragment.

concentration in the reactor as for the heterogeneous reactions. Homogeneous catalysts were removed from the reaction solution before injecting liquid aliquots into a gas chromatograph by passing over a dimethylaminopropyl-modified SiO$_2$ column (∼0.5 g, Aldrich), which adsorbed alkyl hydroperoxides and calixarene−Ti species without altering epoxide concentrations. As discussed elsewhere,[32] epoxidation rates on calixarene−Ti materials depend on reactant and catalyst concentrations as described by

$$\text{rate} = \frac{\partial[\text{epoxide}]}{\partial t} = k[\text{Ti}][\text{alkene}][\text{TBHP}] \qquad (1)$$

in which [Ti] is the total Ti concentration in the reactor, and all concentrations are in moles L^{-1}, resulting in a rate constant k with units of M^{-2} s^{-1}. This rate expression was previously shown to accurately describe reaction rates in the range of reactant concentrations used here. The rate equation and the rate constants were independent of the surface density of Ti on SiO$_2$, consistent with uniform single-site catalytic structures.[32]

Results and Discussion

Spectroscopic Consequences of Support. Calixarene surface densities (from TGA) and Ti surface densities (from ICP/MS) are given in Table 1 for all materials. A ∼1:1 Ti:calixarene molar ratio was measured for all grafted calixarenes and oxide supports, except **1-TiO$_2$**, for which Ti content cannot confirm the concentration of grafted complexes. These surface densities were achieved upon contacting supports with excess calixarene−Ti complexes; similar surface densities on SiO$_2$, TiO$_2$, and Al$_2$O$_3$ indicate that surface concentrations are predominantly limited by the calixarene footprint and not by the number or type of surface defect sites. Surface densities were measured after extensive extraction in hot toluene and therefore represent covalent grafting on SiO$_2$, TiO$_2$, and Al$_2$O$_3$.

Solid-state ^{13}C CP/MAS NMR spectra of grafted materials **1-SiO$_2$**, **1-Al$_2$O$_3$**, and **1-TiO$_2$** (Figure 1) exhibit sharp resonances at 23 ppm and 63−70 ppm, consistent with surface Si,[51] Ti,[51] and Al alkoxides[52] formed from the titanium isopropoxide precursor. Resonances at 30−35 ppm and 120−145 ppm are consistent with the spectrum of calixarene **1a** in solution. Homogeneous complex **1c**, **1-SiO$_2$**, **1-TiO$_2$**, and **1-Al$_2$O$_3$** all possess a resonance at ∼161 ppm due to the calixarene ipso carbon (adjacent to the phenol oxygen), which is shifted
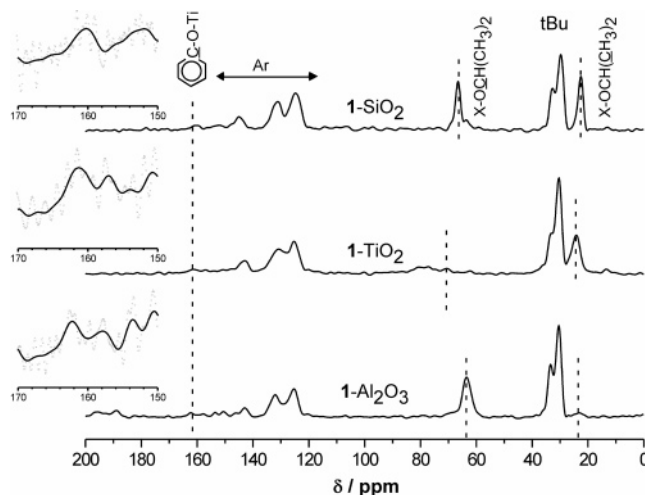

Figure 1. Solid-state ^{13}C CP/MAS NMR spectra of **1-SiO$_2$**, **1-TiO$_2$**, and **1-Al$_2$O$_3$** collected at a spinning rate of 14 kHz. Inset shows 10× magnification of region around ipso carbon resonance at ∼161 ppm. Curves shown result from 20-point finite Fourier transform smoothing of the experimental data to remove high frequency noise.

significantly from the corresponding resonance in the free calixarene ligand **1a** (152 ppm), indicative of calixarene−Ti coordination in all samples. In complexes with additional electron-withdrawing ligands, this resonance is shifted further downfield, as in *tert*-butylphenol-TiCl$_3$ (169 ppm[36]) and calixarene−TiCl **1d** (163 ppm[49]). The calixarene−Ti LMCT edge energies of **1-SiO$_2$**, **1-Al$_2$O$_3$**, and **1-TiO$_2$**, obtained from diffuse-reflectance UV-vis spectroscopy (Figure 2) are all at ∼2.20 eV, irrespective of the identity of the support. Calixarene−TiOPr **1b** and homogeneous calixarene−TiOSiPh$_3$ **1c** also give similar LMCT energies (2.34 and 2.37 eV, respectively, Figure S1). These latter complexes have slightly higher energies because charge separation in the excited state is less favorable in low dielectric solvents (e.g., chloroform) than in high dielectric environments typical of hydroxylated oxide surfaces.[53] The edge energy of calixarene−TiCl **1d** is lower at 1.9 eV.[32] The position of the pre-edge maximum and relative areas of the pre-peaks in the pre-edge region of Ti K-edge (Figure 3, Table 1) for **1c** and **1-SiO$_2$** are the same within the accuracy of the spectra and their analysis. The A2 + A3 area (see Figure 3) in **1-Al$_2$O$_3$** is

(51) Dire, S.; Babonneau, F. *J. Non-Cryst. Solids* **1994**, *167*, 29−36.
(52) Abraham, A.; Prins, R.; van Bokhoven, J. A.; van Eck, E. R. H.; Kentgens, A. P. M. *J. Phys. Chem. B* **2006**, *110*, 6553−6560.
(53) Lever, A. B. P. *Inorganic Electronic Spectroscopy*; Elsevier: New York, 1984. Shepherd, R. E.; Hoq, M. F.; Hoblack, N.; Johnson, C. R. *Inorg. Chem.* **1984**, *23*, 3249−3252.
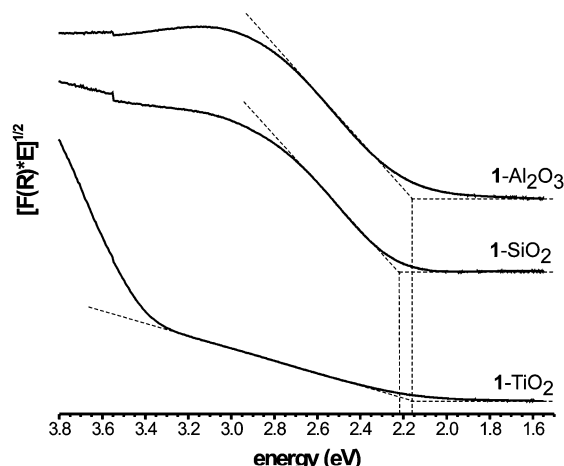
Figure 2. Diffuse-reflectance UV–visible spectra of supported complexes **1**-SiO$_2$, **1**-Al$_2$O$_3$, and **1**-TiO$_2$. All spectra use the Kubelka–Munk formalism and assume the LMCT transition to be indirect. Edge energies are defined as the intercept of the indicated tangent lines, calculated from the first derivative of the transformed spectra.
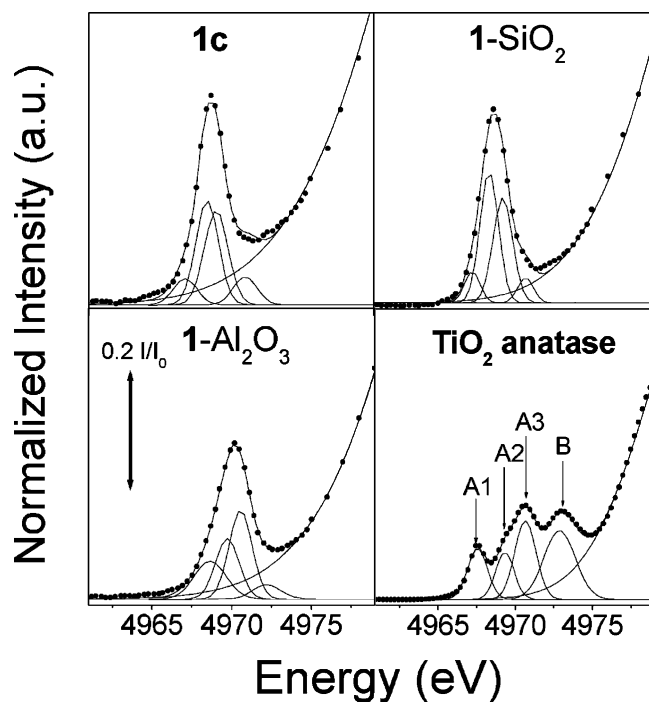

Figure 3. Pre-edge region of Ti K-edge XANES for **1c** and supported complexes **1**-SiO$_2$ and **1**-Al$_2$O$_3$. The spectrum of anatase TiO$_2$, a support material and a representative six-coordinate Ti material, is also shown for comparison. Intensities are normalized with respect to that at 5050−5200 eV. The A2 and A3 feature intensities are a measure of the availability of unoccupied electronic states at the Ti 3d level. For a detailed description about the origin of the four different features, see experimental section and previous reference.[38]

smaller than in **1c** and **1**-SiO$_2$ by ∼0.1 units and appears at higher energies (∼0.4 eV), but this difference is significantly smaller than would indicate an increase in average coordination number from 4 to 5.[38,40] Ti K-edge XANES data were not specific to grafted species in **1**-TiO$_2$ because of the overlapping features and strong contributions from ubiquitous Ti in the support.

The ^{13}C CP/MAS NMR, UV–visible, and XANES Ti K-edge spectra for all materials discussed thus far are similar and quite distinct from those for complexes with deliberate modifications to the Ti inner-sphere. These spectra are therefore consistent

Scheme 3. Steps of Ti-Catalyzed Epoxidation of Alkenes with Alkyl Hydroperoxide, as Described in Text
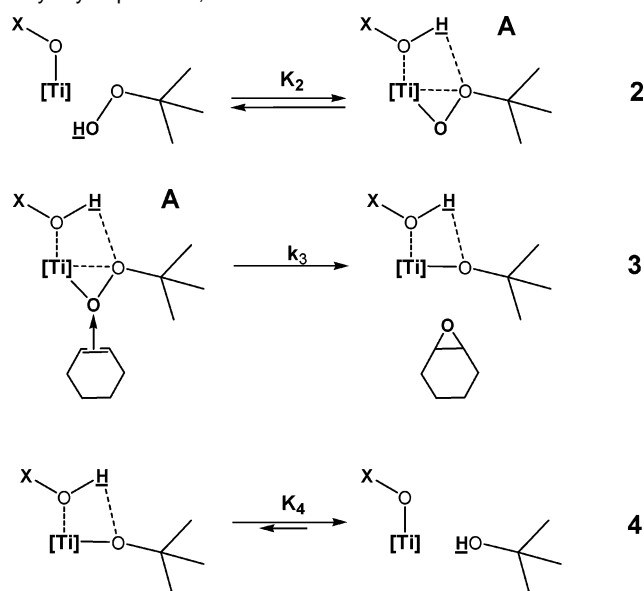
with our assertion that **1**-Al$_2$O$_3$, **1**-TiO$_2$, and **1**-SiO$_2$ all consist of single-site, isolated Ti centers with inner-sphere coordination environments similar to those in soluble compound **1c**. In the absence of outer-sphere effects, which are largely undetectable by these techniques, these four Ti species should give similar epoxidation turnover rates on the basis of previously established quantitative correlations between catalytic reactivity and Ti electronic structure.[38]

Catalytic Consequences of Altering the Support. Alkene epoxidation with hydroperoxides involves equilibrated coordination of hydroperoxides to Ti centers, electrophilic attack by alkenes at O1 oxygens in bound hydroperoxides, and desorption of alcohol coproducts (steps 2, 3, and 4 in Scheme 3).[6,7] The higher rates measured for electron-rich alkenes[4,7,32] and the theoretical estimates of activation barriers for cluster models[14,15] indicate that epoxidation events occur either as the rate-determining step or before it. Thus, the rate constant k, (eq 1) used here to report epoxidation reactivity, is given by $k = k_3 K_2$. These steps have been proposed as a common mechanism on Ti sites in titanosilicates (e.g., TS-1), surface grafted Ti species, and homogeneous silsesquioxanes, which share in common the required isolated Ti centers with 4-fold coordination (discussed above).

The [**Ti**] nomenclature used here is intended to represent the Ti atom and all ligands that remain connected to Ti during kinetically relevant steps; these "static" ligands can be the oxide framework, as in TS-1, an organic ligand, or both. The intermediates are drawn to reflect the expansion of the Ti coordination sphere required for epoxidation.[21] The structure for **A** used in Scheme 3 was proposed by Sinclair and Catlow[12] on the basis of a comparison of density functional theory estimates and measured epoxidation rates for different solvents and additives. The identity of ligand **X** participating in k_3, and therefore the source of the acidic protons involved in stabilizing intermediate **A**, remains unclear.[11−16] Moreover, the group to which the proton is transferred from the hydroperoxide in K_2 is often written as distinct from the species providing the proton-stabilizing intermediate **A**. Scheme 3 allows, but does not require, that these groups be indistinguishable. In this section,
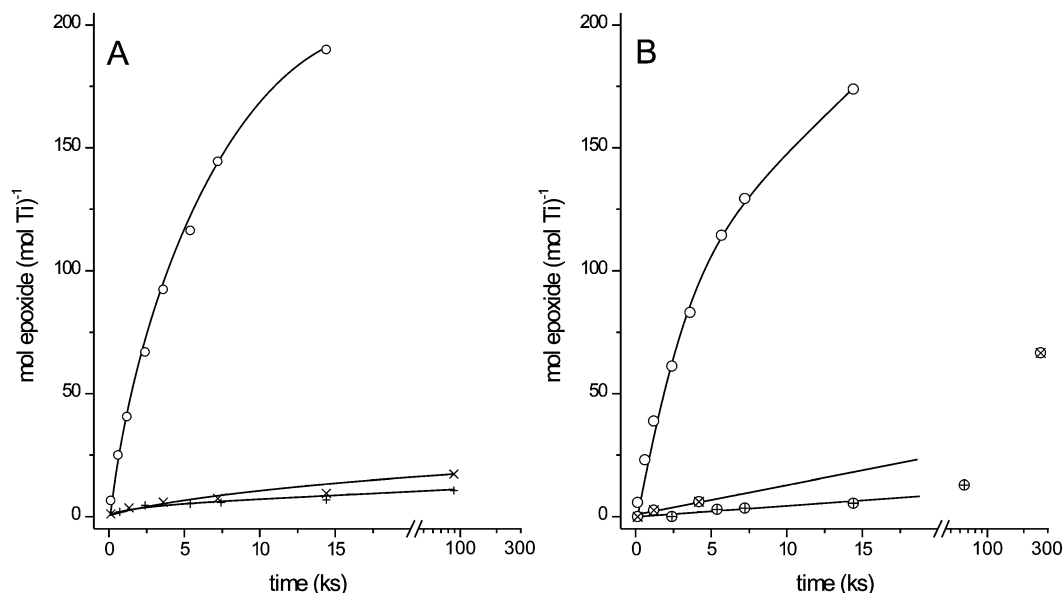
Figure 4. Catalytic turnovers as a function of time for (A) grafted **1**-SiO$_2$ pretreated at 393 K ($k = 6.9$ M^{-2} s^{-1}, O) as compared to homogeneous complexes **1b** ($k = 0.4$ M^{-2} s^{-1}, +) and **1c** ($k = 0.4$ M^{-2} s^{-1}, X), and for (B) grafted **1**-SiO$_2$ ($k = 6.0$ M^{-2} s^{-1}, O), **1**-TiO$_2$ ($k = 0.2$ M^{-2} s^{-1}, ⊗), and **1**-Al$_2$O$_3$ ($k = 0.1$ M^{-2} s^{-1}, ⊕) pretreated at 473 K. Catalytic turnovers are expressed as mol cyclohexene epoxide per mol Ti per s. Rate constants for the homogeneous complexes were calculated for initial four turnovers.

epoxidation rates in soluble calixarene–TiOPr **1b** and calixarene–TiOSiPh$_3$ **1c** complexes are compared to those on grafted **1**-SiO$_2$, **1**-Al$_2$O$_3$, and **1**-TiO$_2$ to probe the catalytic consequences of hydroxylated supports acting as the source of outer-sphere Brønsted acidity for Ti centers that are otherwise electronically similar.

Figure 4a shows that epoxide turnover rates on homogeneous species **1b** and **1c** are similar to each other but ~20 times lower than on **1**-SiO$_2$ treated at 393 K.[54] Complexes **1b** and **1c** also deactivate with time, while **1**-SiO$_2$ is stable (Figure S3). As previously reported for incompletely condensed Ti-silsesquioxanes,[29] these data indicate that Ti–OSi connectivity is, by itself, insufficient for epoxidation catalysis, even though triphenylsilanol ligands can provide steric bulk and electron-withdrawing properties comparable to those for monodentate silsesquioxane ligands or isolated silanols on SiO$_2$[55] and have been previously used as ligands in Ti epoxidation catalysts.[34,56] Figure 4b shows that initial epoxide turnover rates on **1**-TiO$_2$ and **1**-Al$_2$O$_3$ are ~50 times lower than on **1**-SiO$_2$ samples treated similarly. The integrated hydroperoxide selectivity (mol epoxide produced per mol hydroperoxide consumed) is ~35% at ~25% hydroperoxide conversion on **1**-TiO$_2$, which is similar to selectivities measured on **1**-SiO$_2$ for nonactivated alkenes (e.g., *n*-octene).[32] At high conversions, selectivities on **1**-SiO$_2$ are near 100%, indicating that the low apparent selectivities on other samples reflect competing noncatalytic pathways that become apparent for catalysts with low epoxidation reactivity. This noncatalytic hydroperoxide consumption is not significant during the initial stages of reaction, where the reported epoxidation rate constants are measured. Products of other cyclohexane
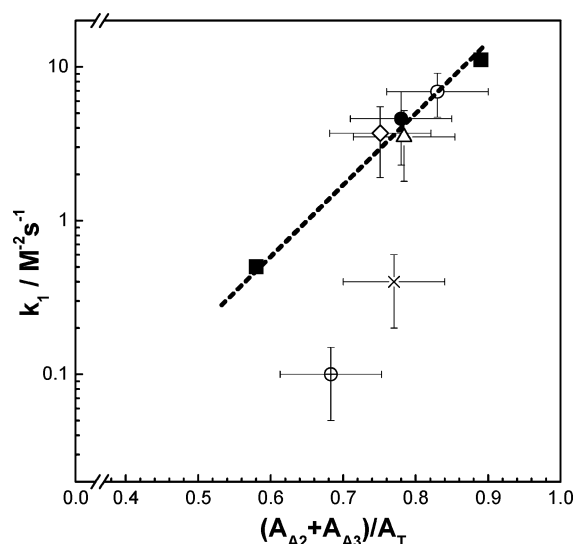
(54) Calixarene–Ti(IV) complexes have been used elsewhere for epoxidation of alkenes (see reference 48): Massa, A.; D' Ambrosi, A.; Pronto, A.; Scettri, A. *Tetrahedron Lett.* **2001**, *42*, 1995–1998.
(55) Duchateau, R.; Cremer, U.; Harmsen, R. J.; Mohamud, S. I.; Abbenhuis, H. C. L.; van Santen, R. A.; Meetsma, A.; Thiele, S. K. H.; van Tol, M. F. H.; Kranenburg, M. *Organometallics* **1999**, *18*, 5447–5459.
(56) Attfield, M. P.; Sankar, G.; Thomas, J. M. *Catal. Lett.* **2000**, *70*, 155–158. Oldroyd, R. D.; Thomas, J. M.; Sankar, G. *Chem. Commun.* **1997**, 2025–2026.

Figure 5. The epoxidation rate constant (pretreated at 393 K, epoxidation of cyclohexene with TBHP, assuming rate eq 1) is plotted against XANES pre-edge component peaks relative area ($A_{A2} + A_{A3})/A_T$ (treated before analysis at 383 K at 10^{-6} Torr, 1 h), for materials **1c** (X), **1**-SiO$_2$ (O), **1**-SiO$_2$-**c** (●), **1**-Al$_2$O$_3$ (⊕), **3**-SiO$_2$ (△), and **4**-SiO$_2$ (◇). The dashed line marks a correlation developed previously[38] that spans all tested 4- and 5-coordinate Ti–SiO$_2$ materials between the two extremes shown (■). This correlation fails to account for the low reactivity of soluble **1c** and **1**-Al$_2$O$_3$, consistent with outer-sphere effects.

oxidation pathways (cyclohexenol and cyclohexenone) were not detected in any of the experiments.

Figure 5 extends our previously reported rate constants for alkene epoxidation as a function of the area of XANES pre-edge features[38] to include those measured on **1**-Al$_2$O$_3$ and **1c**. Turnover rates on these catalysts are ~10 times lower than predicted from Ti centers with the electronic configuration represented by their near-edge X-ray absorption spectra, on the basis of our previous correlations (Figure 5).[38] The similar solid-state NMR and UV spectra for **1**-TiO$_2$ and **1**-Al$_2$O$_3$ indicate that **1**-TiO$_2$ also deviates from the trends shown by the other

catalysts in Figure 5. Thus, we conclude that the low turnover rates measured on **1**-TiO$_2$ and **1**-Al$_2$O$_3$ do not reflect inner-sphere effects on Ti centers caused by these supports acting as monodentate ligands, but instead arise from outer-sphere effects that do not cause detectable changes in the electronic state of Ti centers.

Except in the patent literature,[10] there have been few systematic studies of isolated Ti sites supported on oxides other than SiO$_2$,[57] such as Al$_2$O$_3$[58] or TiO$_2$, which would provide evidence for outer-sphere effects caused by support surfaces. Sol−gel mixed oxides containing TiO$_2$[59] are not well-suited to explore support effects because of their complex and poorly defined Ti environments. Strong Brønsted acids[34,60] open epoxide rings rapidly in the presence of traces of water and lead to low epoxide yields and to deactivation via chelation of Lewis acid active sites by the alkane diols.[61] Cluster density functional theory studies of titanosilicate structures suggest that Ti Lewis centers with vicinal weakly acidic protons form hydrogen-bonded structures such as intermediate **A** (Scheme 3), which decrease the activation barrier for the kinetically relevant step 3 in the catalytic cycle (Scheme 3).[11−15] This decrease in activation barriers is accompanied by a concomitant increase in [**Ti**]O-OR bond lengths and by a decrease in the energy level of the σ^* orbital involved in the O−O bond.[13,15]

These outer-sphere effects caused by protons have been difficult to detect unambiguously in solid oxidation catalysts, but have been more clearly established in homogeneous systems. H-bonding has been implicated in hydroperoxide activation by homogeneous Ti(OSiMe$_3$)$_4$ catalysts in high alkyl hydroperoxide concentrations,[17] by protonated analogues of Ti−salen salts,[62]

and by fluorous alcohols.[63] Higher rates of peroxide heterolytic cleavage on Fe heme-type catalysts correlate with decreasing pK_a of alcohol co-solvents.[64,65] Outer-sphere effects caused by protons also lead to an increase in epoxidation rates when using peroxyacid oxidants,[8] heme enzymes, such as the cytochrome P450 family,[66] and bioinspired non-heme iron catalysts.[67] The "pull" effect of vicinal acid centers in heme enzymes has also been demonstrated in "hangman" metalloporphyrins.[68] Similar effects have been implicated in the accelerating effects of increasingly acidic alcohols in the epoxidation of alkenes with aqueous H$_2$O$_2$ on TS-1.[26,69] On TS-1, reactant solubility also correlates with the pK$_a$ of alcohol cosolvents,[28] but these effects are too weak to account for the strong effects of alcohols on epoxidation rates.[26]

In view of these precedents, the higher epoxidation rates on **1**-SiO$_2$, relative to Ti sites with similar inner-sphere coordination environments in solution or grafted on TiO$_2$ or Al$_2$O$_3$, are attributed to cooperative interactions between Ti Lewis acid sites and weakly acidic protons provided by the SiO$_2$ support. SiO$_2$ surfaces, with a high density of weakly acidic protons, provide adsorbed species with an environment resembling that in high-dielectric solvents with a pK$_a$ of ∼7.[70] Cooperative H-bonding intermediates between organic and inorganic active sites and surface silanols are easily formed.[71] In contrast, the outer-sphere environment in homogeneous **1c** is imposed by octane, a low dielectric aprotic solvent, as demonstrated by the higher energy of the LMCT band (discussed above). Exposure of **1c** to TBHP at concentrations used in our catalytic experiments led to the quantitative formation of free triphenylsilanol ligands (by solution ^{1}H NMR), indicating that large values of K_2 are favored by the weak acidity of the triphenylsilanol ligand (∼2 pK$_a$ units higher than for isolated silanols on SiO$_2$[55]). However, the resulting silanol concentration is many orders of magnitude lower than the concentrations for which alcohols were found previously to alter the rate of heterolytic cleavage of metal-alkylhydroperoxides.[64] The overall epoxidation rate for homogeneous **1c** is therefore determined by a low value of k_3. We have previously observed a correlation between decreasing cyclohexene epoxidation rates for **1**-SiO$_2$ and increasing temperature of catalyst pretreatment,[38] which would decrease silanol densities and the ability to form intermediate **A**.

Fully hydroxylated anatase TiO$_2$ and Al$_2$O$_3$ (e.g., boehmite or steam-treated γ-alumina) surfaces exhibit higher densities of OH groups than SiO$_2$,[72] and, unlike SiO$_2$, protonate ammonia and piperidine, indicating higher acid strength than SiO$_2$.[73] On Ti centers grafted on Al$_2$O$_3$ and TiO$_2$ surfaces, we conclude that intermediate **A** (Scheme 3) is very reactive (large k_3) but present at low concentrations (low K_2) because its formation requires the transfer of a proton from the hydroperoxide to

(57) Gianotti, E.; Bisio, C.; Marchese, L.; Guidotti, M.; Ravasio, N.; Psaro, R.; Coluccia, S. *J. Phys. Chem. C* **2007**, *111*, 5083−5089. Guidotti, M.; Ravasio, N.; Psaro, R.; Ferraris, G.; Moretti, G. *J. Catal.* **2003**, *214*, 242−250. Fraile, J. M.; García, J. I.; Mayoral, J. A.; Vispe, E.; Brown, D. R.; Naderi, M. *Chem. Commun.* **2001**, 1510−1511. Fraile, J. M.; García, J. I.; Mayoral, J. A.; Vispe, E. *Appl. Catal. A:* **2004**, *276*, 113−122.

(58) van Vliet, M. C. A.; Mandelli, D.; Arends, I.; Schuchardt, U.; Sheldon, R. A. *Green Chem.* **2001**, *3*, 243−246. Rinaldi, R.; Schuchardt, U. *J. Catal.* **2004**, *227*, 109−116.

(59) Beck, C.; Mallat, T.; Burgi, T.; Baiker, A. *J. Catal.* **2001**, *204*, 428−439. Hutter, R.; Mallat, T.; Baiker, A. *J. Catal.* **1995**, *153*, 177−189. de Farias, R. F.; Arnold, U.; Martinez, L.; Schuchardt, U.; Jannini, M. J. D. M.; Airoldi, C. *J. Phys. Chem. Solids* **2003**, *64*, 2385−2389.

(60) Iengo, P.; Aprile, G.; Di Serio, M.; Gazzoli, D.; Santacesaria, E. *Appl. Catal. A* **1999**, *178*, 97−109. Gianotti, E.; Oliveira, E. C.; Coluccia, S.; Pastore, H. O.; Marchese, L. *Inorg. Chim. Acta* **2003**, *349*, 259−264.

(61) Davies, L.; McMorn, P.; Bethell, D.; Page, P. C. B.; King, F.; Hancock, F. E.; Hutchings, G. J. *Chem. Commun.* **2000**, 1807−1808. Corma, A.; Domine, M.; Gaona, J. A.; Jordá, J. L.; Navarro, M. T.; Rey, F.; Pérez-Pariente, J.; Tsuji, J.; McCulloch, B.; Nemeth, L. T. *Chem. Commun.* **1998**, 2211−2212.

(62) Sawada, Y.; Matsumoto, K.; Kondo, S.; Watanabe, H.; Ozawa, T.; Suzuki, K.; Saito, B.; Katsuki, T. *Angew. Chem., Int. Ed.* **2006**, *45*, 3478−3480.

(63) van Vliet, M. C. A.; Arends, I.; Sheldon, R. A. *Synlett* **2001**, 1305−1307. van Vliet, M. C. A.; Arends, I.; Sheldon, R. A. *Synlett* **2001**, 248−250. Berkessel, A.; Adrio, J. A.; Huttenhain, D.; Neudorfl, J. M. *J. Am. Chem. Soc.* **2006**, *128*, 8421−8426. Berkessel, A.; Adrio, J. A. *J. Am. Chem. Soc.* **2006**, *128*, 13412−13420.

(64) Traylor, T. G.; Xu, F. *J. Am. Chem. Soc.* **1990**, *112*, 178−186.

(65) Stephenson, N. A.; Bell, A. T. *Inorg. Chem.* **2006**, *45*, 2758−2766. Lee, W. A.; Yuan, L. C.; Bruice, T. C. *J. Am. Chem. Soc.* **1988**, *110*, 4277−4283.

(66) Sono, M.; Roach, M. P.; Coulter, E. O.; Dawson, J. H. *Chem. Rev.* **1996**, *96*, 2841−2887. Ozaki, S. I.; Roach, M. P.; Matsui, T.; Watanabe, Y. *Acc. Chem. Res.* **2001**, *34*, 818−825.

(67) Chen, K.; Costas, M.; Kim, J.; Tipton, A. K.; Que, L. *J. Am. Chem. Soc.* **2002**, *124*, 3026−3035. Taktak, S.; Ye, W.; Herrera, A. M.; Rybak-Akimova, E. V. *Inorg. Chem.* **2007**, *46*, 2929−2942.

(68) Chang, C.-H.; Chng, L. L.; Nocera, D. G. *J. Am. Chem. Soc.* **2003**, *125*, 1966−1976. Dempsey, J. L.; Esswein, A. J.; Manke, D. R.; Rosenthal, J.; Soper, J. D.; Nocera, D. G. *Inorg. Chem.* **2005**, *44*, 6879−6892.

(69) Sato, T.; Dakka, J.; Sheldon, R. A. In *Zeolites and Related Microporous Materials: State of the Art 1994*, Proceedings of the 10th International Zeolite Conference, Garmisch-Partenkirchen, Germany, July 17-22, 1994; Weitkamp, J., Ed.; Elsevier: Amsterdam, Netherlands, 1994; Vol. 84, p 1853−1860.

(70) Rouxhet, P. G.; Sempels, R. E. *J. Chem. Soc., Faraday Trans. 1* **1974**, *70*, 2021−2032. Anderson, J. H.; Lombardi, J.; Hair, M. L. *J. Colloid Interface Sci.* **1975**, *50*, 519−524. Hair, M. L.; Hertl, W. *J. Phys. Chem.* **1970**, *74*, 91−94.

(71) Bass, J. D.; Anderson, S. L.; Katz, A. *Angew. Chem., Int. Ed.* **2003**, *42*, 5219−5222; Bass, J. D.; Solovyov, A.; Pascall, A. J.; Katz, A. *J. Am. Chem. Soc.* **2006**, *128*, 3737−3747.

(72) Knozinger, H. In *The Hydrogen Bond: Recent Developments in Theory and Experiments*; Schuster, P., Zundel, G., Sandorfy, C., Eds.; American Elsevier Pub. Co.: New York, 1976; pp 1267−1353.

(73) Moss, J. H.; Parfitt, G. D.; Wright, A. *Colloid Polym. Sci.* **1978**, *256*, 1121−1130. Busca, G. *Catal. Today* **1998**, *41*, 191−206. Majors, P. D.; Raidy, T. E.; Ellis, P. D. *J. Am. Chem. Soc.* **1986**, *108*, 8123−8129. Tsyganenko, A. A.; Pozdnyakov, D. V.; Filimonov, V. N. *J. Mol. Struct.* **1975**, *29*, 299−318. Tsyganenko, A. A.; Storozheva, E. N.; Manoilova, O. V.; Lesage, T.; Daturi, M.; Lavalley, J. C. *Catal. Lett.* **2000**, *70*, 159−163.

Table 2. Tabulated Values of the Upper Rim (R_2) Group Hammett Inductive Parameter (σ^*),[77] and Monomeric Phenol pK_a[78] [a]

	calixarene[b]	ipso ^{13}C NMR shift (ppm)[c]		$R_2 \sigma^*$	phenol pK_a
	R_2	ligand (**Xa**)	SiO$_2$ complex		(H$_2$O)
1	tBu	151.6	161	−0.3	10.31
2	H	150.6	164	+0.5	9.99
3	(CO)Ph	155.5	167	+2.2	∼9.0
4	NO$_2$	161.2	169	+4.0	7.18

[a] Data for the monomeric phenols are provided in the absence of data on the calixarenes themselves. Data for calixarene **3** are estimated from correlations of pK_a to Hammett constants presented in the cited references. [b] Labeled as per Scheme 1. [c] Considered to be the resonance at lowest field.
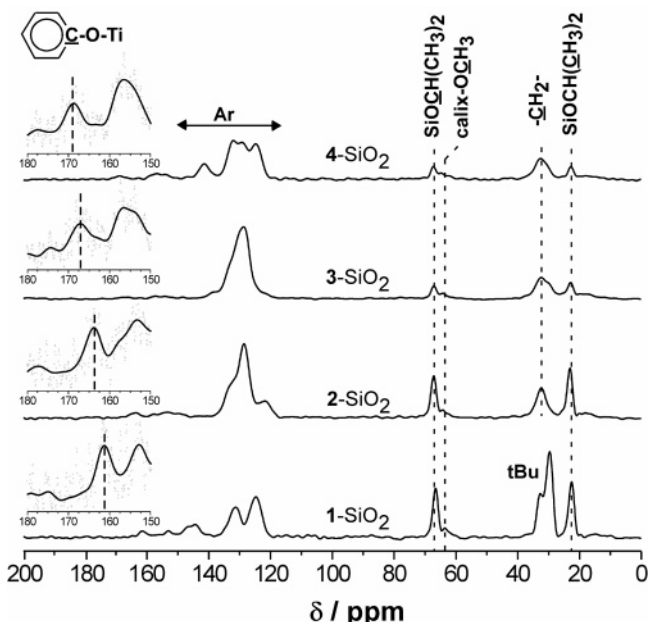
Figure 6. Solid-state ^{13}C CP/MAS NMR spectra of upper-rim modified grafted species collected at a spinning rate of 14 kHz and a contact time of 1.0 ms. A resonance at ∼196 ppm corresponding to carbonyl species in **3**-SiO$_2$ was observed using a contact time of 2.5 ms. Signals are normalized per g of material. Inset shows 10× (20× for **3**-SiO$_2$) magnification of region near ipso carbon resonance and fit with a 20-point finite Fourier transform to remove high frequency noise.

surfaces more acidic than SiO$_2$. These compensating thermodynamic and kinetic factors lead to optimal rates for outer spheres with protons of intermediate acid strengths. These effects are consistent with intermediates resembling **A** in Scheme 3, for which stronger acids would decrease K_2 but concurrently increase k_3. Therefore, rates reflect the value of k_3 for weak acids, for which Ti sites tend to be saturated with bound peroxides; as acid strength increases, peroxide binding weakens and rates become proportional to ($k_3 K_2$) values, which decrease with increasing acid strength. Such "volcano curves" are ubiquitous in catalysis and have been reported previously for mechanistically distinct Pt-based[74] and MoOx-based[75] epoxidation catalysts. However, this behavior has not, to our knowledge, been previously considered in Ti-based epoxidation catalysis.

(74) Pizzo, E.; Sgarbossa, P.; Scarso, A.; Michelin, R. A.; Strukul, G. *Organometallics* **2006**, *25*, 3056−3062.
(75) Shimura, K.; Fujita, K.; Kanai, H.; Utani, K.; Imamura, S. *Appl. Catal. A* **2004**, *274*, 253−257.
(76) Araki, K.; Iwamoto, K.; Shinkai, S.; Matsuda, T. *Bull. Chem. Soc. Jpn.* **1990**, *63*, 3480−3485. Shinkai, S.; Araki, K.; Koreishi, H.; Tsubaki, T.; Manabe, O. *Chem. Lett.* **1986**, 1351−1354.
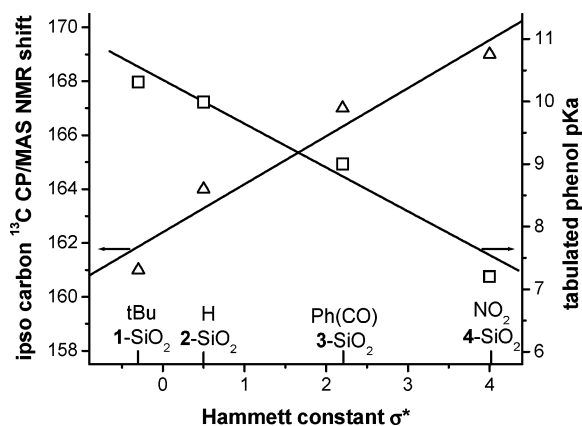
Figure 7. Correlation between observed ipso carbon ^{13}C CP/MAS NMR shifts and tabulated values of the Hammett constant and individual phenol pK_a.
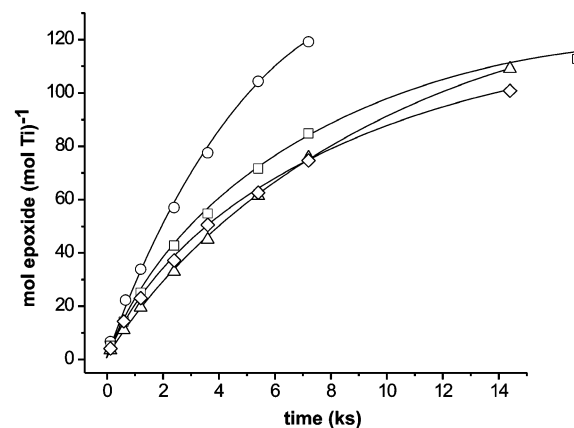

Figure 8. Catalytic turnovers as a function of time for materials **1**-SiO$_2$ (k = 5.8 M^{-2} s^{-1}, O), **2**-SiO$_2$ (k = 4.3 M^{-2} s^{-1}, □), **3**-SiO$_2$ (k = 3.5 M^{-2}s^{-1}, △), and **4**-SiO$_2$ (k = 3.7 M^{-2}s^{-1}, ◇), after pretreatment at 523 K and expressed as mol cyclohexene epoxide per mol Ti per s.

Spectroscopic and Catalytic Consequences of Altering Calixarene Ligands. We next test whether the phenolic groups on the calixarene ligand can create an outer-sphere Brønsted acid effect on epoxidation rates similar to those we have described here for oxide supports. The upper rim groups in calixarene−Ti complexes **1b**−**4b** were chosen to cover a broad range of Hammett constants, from electron-donating (^{t}Bu) to electron-withdrawing (NO$_2$); these systematic modifications are expected to lead in turn to large changes in the pK_a of the calixarene ligand. The tabulated pK_a values for monomeric phenol (Table 2) can be used to provide an upper bound for the respective free calixarenes, because macrocycles stabilize the conjugate base more effectively than phenol monomers.[76]

In lieu of a direct measure of the acidity of the protonated form of the grafted calixarene−Ti complexes, ^{13}C NMR spectra (Figure 6) were used to probe the degree of ligand electron delocalization. In particular, the position of the ipso carbon resonance is sensitive to reactions of free phenols to form Ti-phenolate complexes.[36] In all SiO$_2$-grafted materials, this resonance is shifted downfield by ∼10 ppm (Table 2) from the corresponding free calixarene in solution,[32,49] consistent with calixarene−Ti connectivity in these materials. The resonances for the free ligand and the SiO$_2$-grafted complexes shift further downfield as the macrocycle aromatic π system becomes more electron-deficient (Table 2), as expected from the changes in

Scheme 4. Epoxidation Intermediate **A** for Grafted Calixarene−Ti(IV) Structures Differing in the Destination of the Proton Transferred from the Hydroperoxide
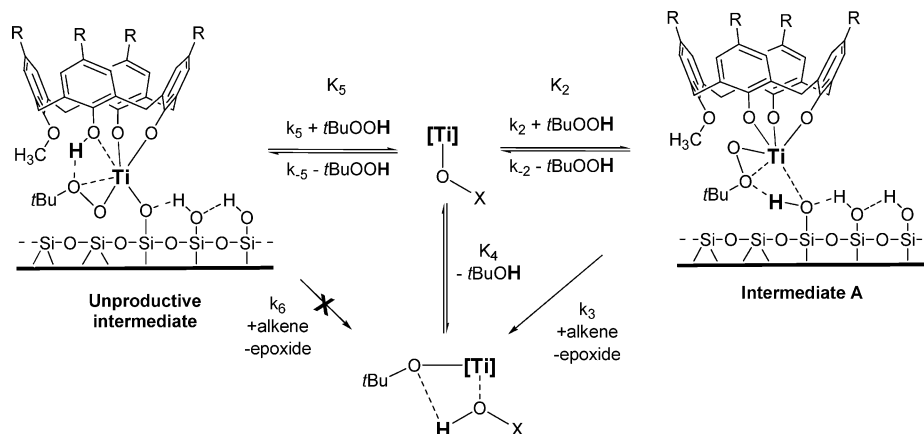
the Hammett constants of the upper rim groups and from the stronger acidity of the respective conjugate phenol (Figure 7). These systematic changes in NMR resonances for the calixarene aromatic π system were not accompanied by significant changes in the energy of ligand-to-metal charge-transfer bands in their UV−visible spectra (Table 1, Figure S4) or in the energy position of the maximum intensity of their pre-edge features in X-ray absorption spectra (Table 1). These findings are consistent with previous theoretical studies,[37] reported NMR spectra,[79] and electrochemical data,[80] which report electronic effects on Ti as a result of changes in phenolate geometry, but not phenolate substituent. This property enables outer-sphere effects of calixarene substituents to be determined independently of concomitant changes in the electronic structure of Ti centers.

Figure 8 shows that epoxide formation turnover rates on **1**-, **2**-, **3**-, and **4**-SiO$_2$ are only weakly influenced by the calixarene upper rim. **1**-SiO$_2$ gave slightly higher rates than **2**-, **3**-, and **4**-SiO$_2$, consistent with weak inner-sphere effects expected from XANES spectra and their correlation with reactivity (Figure 5). These small changes in epoxidation rates with >3 pK_a changes in calixarene phenol acid strength between **1**-SiO$_2$ and **4**-SiO$_2$ suggest that Ti-OCalix bonds are not cleaved in kinetically relevant steps required for epoxidation turnovers. The preferential cleavage of Ti−OCalix bonds over Ti−OSi bonds was previously proposed on the basis of thermodynamic arguments, such as the strained nature and greater number of Ti−OCalix bonds,[32] and of the relative acidity of isolated phenols and silanols. The stoichiometric replacement of alkyl hydroperoxides for alkoxides has been reported for Ti(O^{i}Pr)$_4$ grafted onto SiO$_2$.[81] The data reported here indicate that phenols are either not generated during hydroperoxide binding ($k_5 \ll k_2$, Scheme 4) or are generated only momentarily as minority species leading to a kinetic dead-end (K_5[TBHP] ≪ 1 and $k_6 \ll k_3$, Scheme 4). A large kinetic barrier to Ti−OC cleavage is consistent with previously observed larger losses of Ti−OSi species compared with Ti−OC species during reaction of molecules containing

both groups with SiO$_2$.[82] Scheme 4 summarizes our conclusions that the "static" [**Ti**] core in Scheme 3 represents an intact calixarene−Ti complex, in which Ti−OSi bonds are broken in kinetically relevant intermediates in Ti-catalyzed epoxidation reactions.

Mechanistic Conclusions

The synthesis and grafting of calixarene−Ti complexes onto oxide surfaces can be used to control independently the inner-sphere ligands at active Ti centers and the surrounding outer sphere. In this approach, macrocyclic multidentate calixarenes lead to Ti centers with similar inner-sphere environments, confirmed by UV−visible spectra and pre-edge features at the Ti K-edge. Grafting onto supports, however, places Ti centers in environments where vicinal OH groups differ markedly in acid strength as a result of the Brønsted acid properties of SiO$_2$, TiO$_2$, and Al$_2$O$_3$ supports. These latter outer-sphere effects lead to ∼50-fold changes in epoxidation turnover rates. The absence of comparable catalytic consequences when altering the pK_a of calixarene ligands via changes in their upper rim lead us to conclude that the single Ti−OSi bond (instead of any of the three Ti-OCalix bonds) is cleaved in kinetically relevant epoxidation steps on Ti−SiO$_2$.

Epoxidation rates increased as homogeneous **1c** was grafted onto SiO$_2$ (**1**-SiO$_2$), and rates were observed previously to increase for mild pretreatment temperatures that would retain the high local hydroxyl surface density on SiO$_2$. We attribute both effects to an increase in the rate of O transfer from Ti-hydroperoxide complexes to alkenes (k_3) via cooperative H-bonding assemblies (intermediate **A**) between Ti centers and vicinal weakly acidic protons. We note that because of the high densities of OH groups pre-existing on these SiO$_2$ surfaces, the SiOH generated by Ti−OSi bond breaking is not required to be the same SiOH involved in increasing k_3, but the two groups are thermodynamically indistinguishable. These H-bonded structures also lead to rapid and thermodynamically favored regrafting of Ti intermediates onto the SiO$_2$ surface following O transfer to the alkene, consistent with the observed lack of

(77) Dean, J. A. *Lange's Handbook of Chemistry*, 15th ed.; McGraw-Hill, Inc.: New York, 1999.
(78) Rived, F.; Roses, M.; Bosch, E. *Anal. Chim. Acta* **1998**, *374*, 309−324.
(79) Harrod, J. F.; Taylor, K. R. *Inorg. Chem.* **1974**, *14*, 1541−1545.
(80) Fussing, I. M. M.; Pletcher, D.; Whitby, R. J. *J. Organomet. Chem.* **1994**, *470*, 109−117.Chen, L. X.; Rajh, T.; Wang, Z. Y.; Thurnauer, M. C. *J. Phys. Chem. B* **1997**, *101*, 10688−10697.
(81) Bouh, A. O.; Rice, G. L.; Scott, S. L. *J. Am. Chem. Soc.* **1999**, *121*, 7201−7210.
(82) Jarupatrakorn, J.; Tilley, T. D. *J. Am. Chem. Soc.* **2002**, *124*, 8380−8388.

(83) Corma, A.; Camblor, M. A.; Esteve, P.; Martinez, A.; Perez-Pariente, J. *J. Catal.* **1994**, *145*, 151−158. Camblor, M. A.; Costantini, M.; Corma, A.; Gilbert, L.; Esteve, P.; Martinez, A.; Valencia, S. *Chem. Commun.* **1996**, 1339−1340.
(84) Imamura, S.; Nakai, T.; Utani, K.; Kanai, H. *J. Catal.* **1996**, *161*, 495−497.

leaching of active structures during epoxidation catalysis on grafted calixarene−Ti complexes.[32] In TS-1 and related materials, silanols formed during synthesis or by hydroperoxide binding can form the required H-bonded intermediate **A** (akin to structures shown in Scheme 4); the low concentrations of pre-existing OH defect sites and the restricted mobility of Ti centers in these materials, however, decrease the likelihood that these structures form. Then, protic solvents with increasing pK_a can bridge silanols and Ti active sites and create the requisite H-bonded intermediate **A** and, in this manner, increase epoxidation turnover rates.[15,26]

Epoxidation rates decrease when stronger acid sites inhibit the formation of H-bonded intermediates (K_2). The lower epoxidation turnover rates on Al-containing Ti-silicates may reflect, in part, the presence of strong Brønsted acids,[83] which destabilize intermediate **A** (decrease K_2). Similarly, the unreactive nature of **1**-TiO$_2$ catalysts indicates that the unreactive nature of Ti centers in anatase TiO$_2$ and Ti−SiO$_2$ with high Ti contents[19,84] reflects the unfavorable equilibrium dictated by low K_2 values, even though coordinatively unsaturated Ti centers are present on surfaces of small anatase crystallites.[85] We conclude that a "volcano"-type relationship leads to optimal epoxidation turnover rates at intermediate acid strengths of vicinal protons, which maximize the values of the relevant ($k_3 \cdot K_2$) product that determines epoxidation rates.

The grafting of catalytic entities with uniform structure onto oxide supports extends the range of outer-sphere environments accessible with protic cosolvents and represents a novel route to tune and to probe the function of active Ti centers. The range of acid strengths and their high density of surface species make oxide surfaces well-suited to promote the cooperative behavior between active sites and acidic protons[2] observed for condensation[71] and hydrogenation[86] reactions. The data and conclusions reported here illustrate how outer-sphere protons positioned by supports also influence epoxidation rates on Ti centers with otherwise identical electronic properties. As a result, an accurate description of the structure and function of inorganic catalysts such as TS-1 and Ti−SiO$_2$ requires that we include outer-sphere effects that complement inner-sphere effects intrinsic to Ti centers and their catalytic properties.

Supporting Information Available: ¹H, ¹³C, and ²⁹Si NMR resonances, FAB-MS, and elemental composition for **1c** and **2c**; UV−visible spectra of homogeneous calixarene−Ti complexes **1b** and **1c** (Figure S1); a correlation between Ti surface densities determined by Ti ICP/MS, calixarene surface densities determined by TGA, and ¹³C CP/MAS NMR intensities for resonance corresponding to calixarene methylene bridges (Figure S2); linearized form of epoxide production vs time for **1b**, **1c**, **1**-SiO$_2$, and **1**-Al$_2$O$_3$ showing stable rate constants for grafted catalysts (Figure S3); UV−visible spectra of upper-rim modified calixarene−Ti materials **1**−**4** on SiO$_2$ (Figure S4); extended comparison of grafted calixarene−Ti catalyst **1**-SiO$_2$ with sequentially assembled calixarene and Ti materials and calcined Ti−SiO$_2$ catalysts including synthesis (Scheme S1), UV−visible spectroscopic comparison (Figure S5), and comparison of catalytic turnovers to epoxide (Figure S6). This material is available free of charge via the Internet at http://pubs.acs.org.

JA074614G

(85) Chen, L. X.; Rajh, T.; Jager, W.; Nedeljkovic, J.; Thurnauer, M. C. *J. Synchrotron Rad.* **1999**, *6*, 445−447.

(86) Pugin, B.; Landert, H.; Spindler, F.; Blaser, H. U. *Adv. Synth. Catal.* **2002**, *344*, 974−979. Gonzalez-Arellano, C.; Corma, A.; Iglesias, M.; Sanchez, F. *Adv. Synth. Catal.* **2004**, *346*, 1316−1328. Goettmann, F.; Boissiere, C.; Grosso, D.; Mereier, F.; Le Floch, P.; Sanchez, C. *Chem. Eur. J.* **2005**, *11*, 7416.